

Threshold Value of DC Array Current and DC String Voltage for Fault Detection in Grid-Connected Photovoltaic System

Nurmalessa Muhammad^{1,4*}, Nor Zaini Zakaria^{2,4}, Sulaiman Shaari^{2,4}, Ahmad Maliki Omar^{3,4}

¹Faculty of Applied Sciences, Universiti Teknologi MARA, UiTM Cawangan Negeri Sembilan, Malaysia

²Faculty of Applied Sciences, Universiti Teknologi MARA, Shah Alam, Malaysia

³Faculty of Electrical Engineering, Universiti Teknologi MARA, Shah Alam, Malaysia

⁴Green Energy Research Center(GERC), Universiti Teknologi MARA, Shah Alam, Malaysia

*Corresponding author's e-mail: nurmalessa@uitm.edu.my

Received: 26 July 2019

Accepted: 11 February 2020

Online First: 29 February 2020

ABSTRACT

The failure detection in a grid-connected photovoltaic (PV) system has become an important aspect of solving the issue of the reduced energy output in the PV system. One of the methods in detecting failure is by using the threshold-based method to compute the ratio of actual and predicted DC array current and DC string voltage value. This value will be applied in the failure detection algorithm by using power loss analysis and may reduce the time, cost and labour needed to measure the quality of the energy output of the PV system. This study presented the threshold value of DC array current and DC string voltage to be implemented in the algorithm of fault detection in grid-connected photovoltaic (PV) system under the Malaysian climate. Data from the PV system located at Green Energy Research Center (GERC) was recorded in 12 months interval using the monocrystalline PV modules. The actual data was recorded using five minutes interval for 30 consecutive days. The prediction of the data was calculated using the mathematical method. The threshold value was determined from the ratio between actual and predicted data. The results show that the DC array current threshold value, σ is 0.9816. While, DC string voltage threshold value, λ is 0.9261. The proposed value may be beneficial for the determination of threshold value for regions with the tropical climate.



Keywords: *threshold value, DC array current, DC string voltage, photovoltaic*

INTRODUCTION

Photovoltaic is a technology that converts solar energy into electrical energy. Many factors are affecting the output of the PV system such as solar irradiance, temperature, soiling and shading. The amount of solar irradiance received, and temperature experienced by a PV device are the main parameters that have dominated the major effect. Other key factors that affect electrical output are partial shading and soiling. Thus, it is very important to take into consideration these factors in PV installation even in the sunny region such as Malaysia [1].

In the context of PV application, currently, the total capacity of PV systems installed in Malaysia is approximately 380.24 MW [2]. Due to these circumstances, the PV systems may face major challenges such as soiling, inverter or balance-of-system component faults, and partial shading [3]. The overall energy output is reduced as a result of PV faults. Furthermore, some faults may further lead to safety and health risk to the personal and the PV system itself. According to Firth, Lomas and Rees (2010) [4], a loss of output from a PV system up to 18% per year is significant.

The fault detection in PV system may overcome the issue of reduced optimum energy output. This failure detection technique may be combined with other methods such as threshold-based technique [5], statistical techniques [6] and artificial intelligent techniques [7]. Currently, numerous identification techniques may be used for possible faults detection in PV systems.

Chouder and Silvestre (2010) [8] has proposed an automatic fault detection method based on the power losses analysis. This method can identify four different types of faults such as faulty modules in a string, faulty string, false alarm and combined faults such as partial shadow, ageing, and MPPT error. However, this method can detect defects that occur only on the DC side of the PV system. Even so, with further enhancement, this

method could be used to identify faulty in the AC side of the PV system. This analytical method is integrated with the failure detection algorithm and threshold-based method to find the fault in the PV system with less amount of time. This threshold diagnosis is the most fundamental issue on the detection of a failure in the PV system [8]. In Malaysia, generally, there is still a lack of study on finding the reliable threshold of DC array current and DC string voltage to be used in the calculation of failure algorithm [9]. The threshold-based method is the comparison of current and voltage indicators with their threshold values [5], [8], [10]–[12]. Hence, the development of a fault detection method for the PV array faults is important for improving the energy conversion efficiency of the PV system, increasing the life span of the PV modules, and reducing maintenance cost [13], [14]. In this study, the new threshold value for DC array current and DC string voltage are presented. This value is crucial for the calculation of DC array current ratio and DC string voltage ratio acceptable range. It is important to be implemented in the failure detection algorithm using power loss analysis integrated with the threshold-based method.

METHODS

This research was conducted at the GERC, Universiti Teknologi MARA Shah Alam. The PV array uses monocrystalline solar modules. The PV system built-in data logger was recorded in a five-minute interval for the optimal monitoring of data quality. The data was recorded for 30 consecutive days. The data was first recorded in April 2012 and was replicated in April 2013. The gap of 12 months was purposely set between two data intervals in capturing the changes of the actual data. Figure 1 shows the location of the PV systems (Latitude 3.1 °N, Longitude 101.5 °E). The first data was recorded after the PV system was installed.

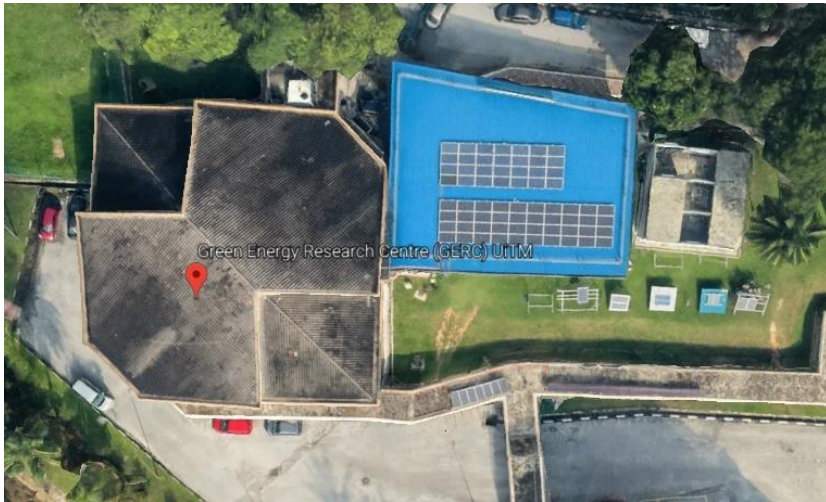


Figure 1: Location of GERC, Kompleks Teratai 1, UiTM, Shah Alam, Malaysia (Latitude 3.1 °N, Longitude 101.5 °E) (Source: Google Maps)

In order to calculate the threshold value, a mathematical approach was used to determine the predicted values for the DC array current and DC string voltage. A statistical approach was used to determine the ratio and the fitness of the prediction value. The predicted DC array current and DC string voltage were determined with Equation (1) and Equation (2), respectively [15]:

$$I_{dc} = I_{mp} \times f_{temp_imp} \times N_P \times f_{dirt} \times f_{mm} \times \frac{G}{1000} \quad (1)$$

$$V_{dc} = (V_{mp} \times f_{temp_vmp} \times N_s) \times \left[1 + k \ln \ln \left(\frac{G}{1000} \right) \right] \quad (2)$$

Where I_{mp} is the current at maximum power of PV array at STC, and the total number of PV strings that connect in parallel is represented as N_P ; f_{temp_imp} and f_{temp_pmp} is the temperature de-rating factor; V_{DC} is the maximum power condition output of voltage of the PV array at STC; k is the constant obtained by curve fitting techniques to acquire the desired point; N_s represents the number of PV modules connected in series; and G denoted as solar irradiance.

This study is defined by two indicators of the divergence which are the DC variables concerning the simulated ones to separate the inappropriate function detected and determining the types of failure. The definition of DC array current ratio, R_c is given in Equation (3) and DC string voltage ratio, R_v in Equation (4) [8]:

$$R_c = \frac{I_{DC_actual}}{I_{DC_predict}} \quad (3)$$

$$R_v = \frac{V_{DC_actual}}{V_{DC_predict}} \quad (4)$$

The type of fault was identified by analysing signal failure and the current or voltage ratios. For the classification stage, R_c and R_v proposed by Chouder and Silvester model were used for determining the type of fault. This study defined the value of σ as the threshold value for DC array current ratio and λ as the threshold value for DC string voltage ratio. Besides, the definition of the thresholds for each monitored parameter, compare the measured value to threshold limits (lower and upper limits) to decide between normal or fault condition.

By following the flowchart that appears in Figure 2, certain failures can be found [8]. Y is denoted as yes, while N is denoted as no.

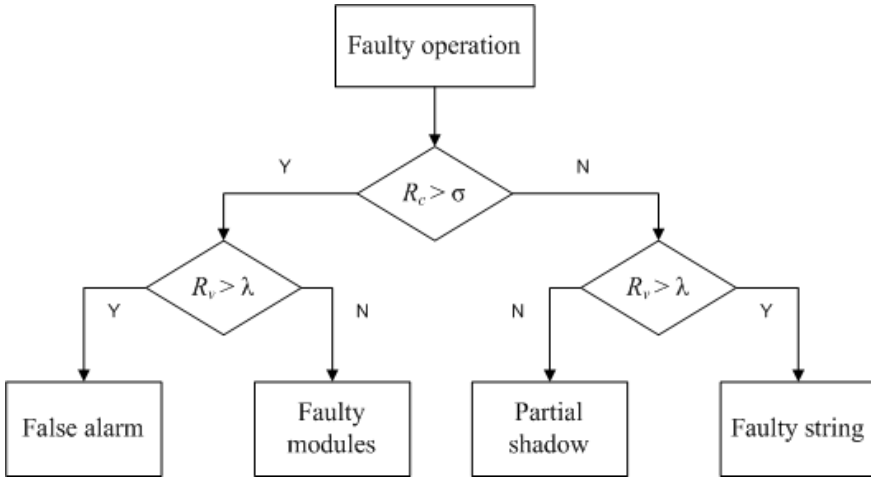


Figure 2: Flowchart of the Failure Classification Procedure

Firstly, a graph of the solar irradiance as a function of module temperature (T_m) was plotted and the value of module temperature when the solar irradiance at 1000 W/m^2 is found. The optimum value of the module temperature was obtained when solar irradiance is at 1000 W/m^2 .

Secondly, a graph of the actual and predicted value of DC string voltage as a function of T_m was plotted. It was found that the values of the actual and predicted DC string voltage is obtained by referring to the value of module temperature from Step 1. This step is crucial to find the ratio of DC string voltage, R_v .

Finally, a graph of the actual and predicted value of DC array current as a function of solar irradiance was plotted. It was found that the values of the actual and predicted DC array current was obtained by referring to the value of solar irradiance at 1000 W/m^2 . From this step, the ratio of DC array current, R_c was found.

RESULTS AND DISCUSSION

Figure 3 shows the solar irradiance as the dependent variable (y-axis) and module temperature as the independent variable (x-axis) for monocrystalline PV system graph. The empirical model for the regression line can be expressed as in Equation (5). Hence, the value of T_m denoted as module temperature with 62.5536 oC was taken when G at 1000 W/m². The decision to take G as 1000 W/m² as the reference point is due to the typical peak value on a terrestrial surface facing the sun on a clear day around solar noon at sea level and used as a rating condition for PV modules and arrays [16].

$$G=0.386(T_m)^2 - 8.1594(T_m) \quad (R^2=0.8183) \quad (5)$$

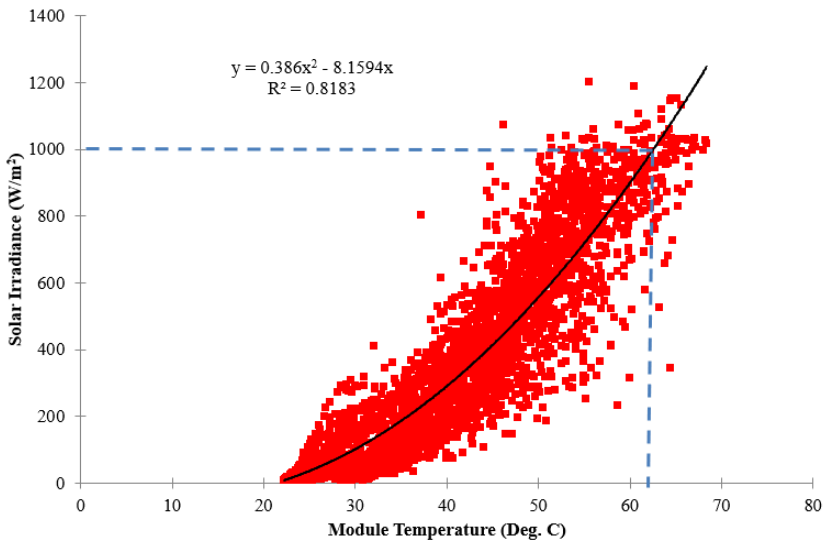


Figure 3: Solar Irradiance as a Function of Module Temperature for Monocrystalline PV Module Graph

Figure 4 shows the graph of the DC array current as a function of solar irradiance. It is observed that the regression lines have a significant difference. The regression line for the polynomial fit of actual 2012 DC array current (blue line) is almost the same with the regression line of polynomial fit of actual 2013 DC array current (pink line). A slight difference may be seen due to the derating factor, such as the module temperature on particular

data is lower as compared to the data a year before. This behaviour was expressed by:

$$I_{dc_2012} = 0.00095364(G) + 0.003904 \quad (R^2 = 0.9834) \quad (6)$$

$$I_{dc_2013} = 0.00096199(G) - 0.00031693 \quad (R^2 = 0.9715) \quad (7)$$

Where,

I_{DC_2012} = MPPT 1 Monocrystalline DC array current for April 2012

I_{DC_2013} = MPPT 1 Monocrystalline DC array current for April 2013

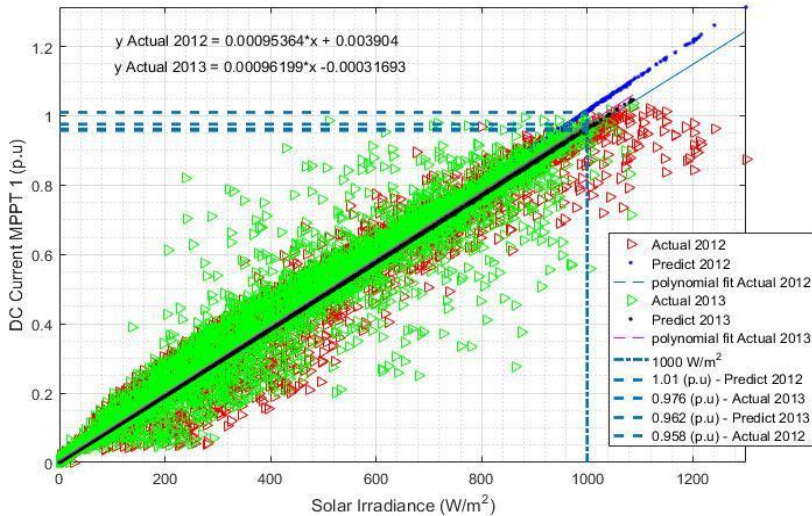


Figure 4: Actual and Measured Values of DC Array Current versus Solar Irradiance for the Year of 2012 and 2013

The trend lines for the DC string voltage is depicted in Figure 5. The trend line of polynomial fit of actual 2012 DC string voltage (blue line) is much higher than the trend line of polynomial fit of actual 2013 (pink line). It may be due to the derating factor such as the cable loss. The behaviour was expressed by:

$$I_{dc_2012} = 0.00095364(G) + 0.003904 \quad (R^2 = 0.9834) \quad (6)$$

$$I_{dc_2013} = 0.00096199(G) - 0.00031693 \quad (R^2 = 0.9715) \quad (7)$$

Where,

I_{DC_2012} = MPPT 1 Monocrystalline DC array current for April 2012

I_{DC_2013} =MPPT 1 Monocrystalline DC array current for April 2013

Referring to the Equation (6) and Equation (7), the value of Monocrystalline DC string voltage when T_m at 62.5536 oC is 0.798 (p.u) and 0.789 (p.u) respectively. Table 1 shows the threshold value for both R_c and R_v . The result shown is for the tropical climate conditions. Hence, these results cannot be compared to the previous study due to the different climate region. Therefore, it is not suitable to compare both regions. In future research, the study should include more data from the PV system installation sites in the country. As a result, it will give a significant input for the threshold values for the Malaysian climate.

Table 1: Threshold Value for DC Array Current and DC String Voltage

Year	The ratio of DC array current (p.u), R_c				The ratio of DC string voltage (p.u), R_v			
	Actual	Predicted	Ratio	Mean, σ	Actual	Predicted	Ratio	Mean, λ
2012	0.958	1.01	0.9485	0.9816	0.798	0.836	0.9545	0.9261
2013	0.976	0.962	1.0146		0.789	0.879	0.8976	

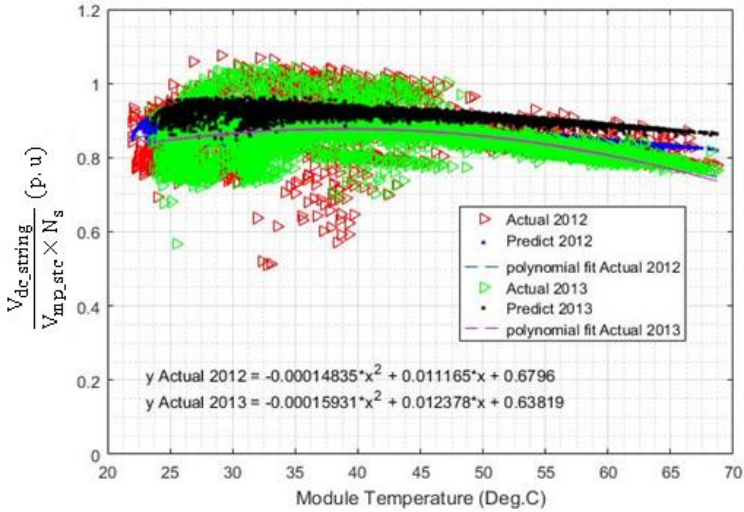


Figure 5: Actual and Measured Values of DC String Voltage as a Function of Solar Irradiance for the Year of 2012 and 2013

CONCLUSION

In this work, a new threshold value for DC array current and DC string voltage for failure detection algorithm of the GCPV system were presented. The method is based on the evaluation of DC array current and DC string voltage indicators. Based on the results, the value of threshold value for DC array current, σ is 0.9816 with minimum and maximum limits of 0.9485 to 1.0146. The threshold value of DC string voltage, λ is given as 0.9261 with minimum and maximum limit of 0.8976 to 0.9545.

ACKNOWLEDGEMENT

The authors would like to thank directly and indirectly to GERC and UiTM for the data available and KPT for funding the SLAB/SLAI scholarship for this study.

REFERENCES

- [1] H. Zainuddin, S. Shaari, A. M. Omar, and M. Z. Hussin, 2013. Modelling of operating temperature for thin film modules for free-standing systems in Malaysia in 2013 IEEE Conference on Clean Energy and Technology (CEAT), Langkawi, pp. 455–460. DOI: 10.1109/CEAT.2013.6775675
- [2] SEDA Malaysia, “Annual Report,” 2017. Accessed from <http://www.seda.gov.my/download/seda-annual-report/>
- [3] S. Spataru, D. Sera, T. Kerekes, and R. Teodorescu, 2013. Photovoltaic array condition monitoring based on online regression of performance model in 2013 IEEE 39th Photovoltaic Specialists Conference (PVSC), Tampa, USA, pp. 0815–0820. DOI: 10.1109/PVSC.2013.6744271
- [4] S. K. Firth, K. J. Lomas, and S. J. Rees, 2010. A simple model of PV system performance and its use in fault detection. *Solar Energy*, 84(4), pp. 624–635. <https://doi.org/10.1016/j.solener.2009.08.004>
- [5] W. Chine, A. Mellit, A. M. Pavan, and S. A. Kalogirou, 2014. Fault detection method for grid-connected photovoltaic plants. *Renewable Energy*, 66, pp. 99–110, 2014. <https://doi.org/10.1016/j.renene.2013.11.073>
- [6] M. Mansouri, M. Hajji, M. Trabelsi, and M. Faouzi, 2018. An effective statistical fault detection technique for grid connected photovoltaic systems based on an improved generalized likelihood ratio test. *Energy*, 159, pp. 842–856. <https://doi.org/10.1016/j.energy.2018.06.194>
- [7] S. Leva, M. Mussetta, and E. Ogliari, 2019. PV Module Fault Diagnosis Based on Microconverters and Day-Ahead Forecast. *IEEE Transactions on Industrial Electronics*, 66(5), pp. 3928–3937. DOI: 10.1109/TIE.2018.2879284

- [8] A. Chouder and S. Silvestre, 2010. Automatic supervision and fault detection of PV systems based on power losses analysis. *Energy Conversion and Management*, 51(10), pp. 1929–1937. <https://doi.org/10.1016/j.enconman.2010.02.025>
- [9] M. Almaktar, H. A. Rahman, M. Y. Hassan, and I. Saeh, 2013. Artificial neural network-based photovoltaic module temperature estimation for tropical climate of Malaysia and its impact on photovoltaic system energy yield. *Progress in Photovoltaics Research and Applications*, 23(3), pp. 659–676. <https://doi.org/10.1002/pip.2424>
- [10] S. Silvestre, M. A. Da Silva, A. Chouder, D. Guasch, and E. Karatepe, 2014. New procedure for fault detection in grid connected PV systems based on the evaluation of current and voltage indicators. *Energy Conversion and Management*, 86, pp. 241–249. <https://doi.org/10.1016/j.enconman.2014.05.008>
- [11] S. Silvestre, A. Chouder, and E. Karatepe, 2013. Automatic fault detection in grid connected PV systems. *Solar Energy*, 94, pp. 119–127. <https://doi.org/10.1016/j.solener.2013.05.001>
- [12] N. Gokmen, E. Karatepe, B. Celik, and S. Silvestre, 2012. Simple diagnostic approach for determining of faulted PV modules in string based PV arrays. *Solar Energy*, 86(11), pp. 3364–3377. <https://doi.org/10.1016/j.solener.2012.09.007>
- [13] S. Vergura, 2018. Hypothesis tests-based analysis for anomaly detection in photovoltaic systems in the absence of environmental parameters. *Energies*, 11(3), p. 485. DOI: 10.3390/en11030485
- [14] L. Chen, S. Li, and X. Wang, 2018. Quickest Fault Detection in Photovoltaic Systems. *IEEE Transactions on Smart Grid*, 9(3), pp. 1835–1847. DOI: 10.1109/TSG.2016.2601082
- [15] A. M. Omar, S. Shaari, and S. I. Sulaiman, SEDA MALAYSIA Grid Connected Photovoltaic Power Systems Design. 2012.

- [16] J. Dunlop, “Solar Radiation Terminology & Definitions, Geometric & Atmospheric Effects, Solar Power & Energy, Measurements & Data.” p. Chapter 2, 2012.